Chapter 1

Introduction

Table of Contents

1-1 Molecular Architecture

The molecular architecture impacts the chemical and physical properties of all polymers. In principle, there are infinitely many possible polymer architectures — that is, infinitely many ways to connect polymer chains. In practice however, long-standing synthetic challenges limit the scope of architectural design. These limitations preclude studies of fundamental physical phenomena as well as potential applications in functional materials. This thesis presents our work to close the design, synthesis, and characterization gaps for bottlebrush polymers, a unique molecular architecture.

This chapter will first introduce the bottlebrush architecture (Section 1-1). The need for improved synthetic methods and systematic structure-property studies will be emphasized. We will then review existing synthetic routes and highlight our approach: living grafting-through ring-opening metathesis polymerization (ROMP) (Section 1-2). Section 1-3 will build complexity by introducing bottlebrush block polymers and discussing the impacts of architecture on self-assembly. Lastly, Section 1-4 will outline the structure of this thesis by connecting these themes of molecular architecture and materials design.

Bottlebrush polymers are a class of graft polymers, which feature a polymer backbone bearing grafted polymer side chains. Compared to linear homopolymers (the simplest possible architecture), bottlebrush polymers display unique properties and introduce new opportunities for molecular shaping. For a fixed monomer chemistry, linear

homopolymers feature only one independent structural parameter: the total degree of polymerization, N (Figure 1.1). In comparison, bottlebrush polymers feature *four* independent parameters: (1) the backbone degree of polymerization, N_{bb}; (2) the side chain degree of polymerization, N_{sc}; (3) the grafting density, z (defined as the average number of grafts per backbone repeat unit); and (4) the distribution of grafts along the backbone (uniform, tapered, etc.) (Figure 1.1). Bottlebrush polymers are primarily distinguished from other graft polymers by high z.

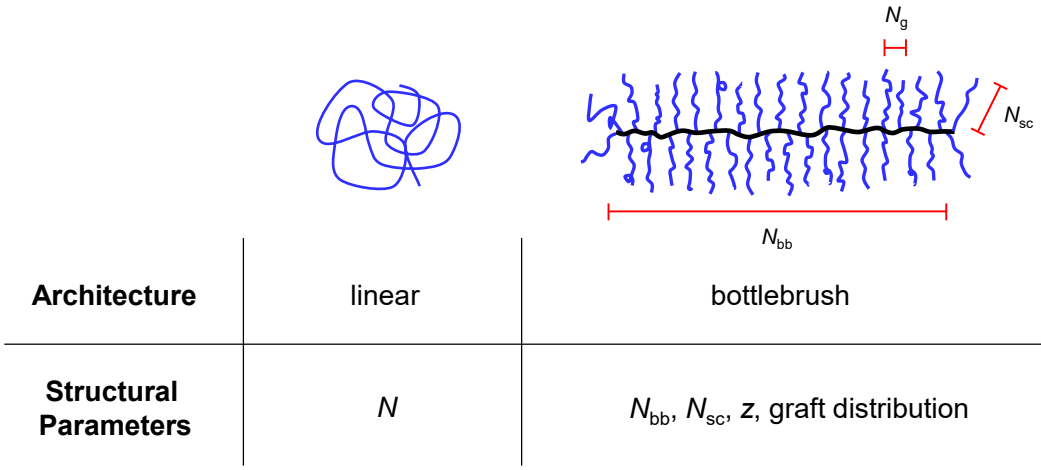

Figure 1.1: Comparison of linear (*left*) and bottlebrush (*right*) polymer architectures. For a fixed monomer chemistry, the linear polymers feature one independent structural parameter: the total degree of polymerization, N. In contrast, bottlebrush polymers must be described by multiple parameters, including the backbone length (N_{bb}), side chain length (N_g), grafting density ($z = 1/N_g$), and graft distribution.

Whereas the conformation of a linear homopolymer can be largely anticipated based on N, the conformation of a bottlebrush polymer depends on the complex interplay of N_{bb}, N_{sc}, z, and the graft distribution. Polymer conformations represent the molecular basis for predicting and controlling all of the physical properties of polymers: therefore, understanding the connections between molecular architecture and polymer conformation is crucial from the perspectives of both fundamental theory and materials design.

In bottlebrush polymers, strong steric repulsion between the side chains imparts a certain bending rigidity to the backbone, causing the brush to adopt an extended, wormlike conformation.[1-2] Due to their extended conformations, bottlebrush polymers display different physical properties than linear analogues. For example, the bottlebrush architecture suppresses entanglements in the melt and lowers the melt viscosity,[3-5] thereby introducing

processing advantages and new opportunities for materials design. Recent reports have exploited these unique properties in the context of supersoft elastomers, [6-8] leading to solvent-free materials with moduli as low as 100 Pa and tensile strains-at-break up to 800%.[9] These properties are direct consequences of the bottlebrush architecture. (In comparison, linear polymers of the same chemical composition have moduli greater than 10^6 Pa and strains-at-break only up to 200%.[9]) In addition to supersoft elastomers, bottlebrush polymers have been developed as rheological modifiers,[10] nanoporous materials,[11-12] solid electrolytes,[13-15] and photonic bandgap materials.[16-18]

Despite the importance of polymer conformation and the rich potential of bottlebrush materials, there is a current lack of consensus regarding many key structure-property relationships. This lack of consensus is due in large part to the challenges associated with capturing the complex interplay of all structural parameters. Table 1.1 provides one example. The influence of N_{sc} on the stiffness of the backbone (expressed as the backbone persistence length, λ_b) is considered. Even for this fundamental relationship, experiments, theory, and computer simulations have proposed many conflicting expressions. Considering the general expression $\lambda_b \sim N_{sc}^{\nu}$, the proposed scaling exponents vary over a wide range: $3/4 \leq \nu \leq 2$.

Table 1.1: Expressions for the relationship between the backbone stiffness (λ_b) and side chain degree of polymerization (N_{sc}). All expressions are provided for densely grafted bottlebrush polymers in a good solvent for the side chains. Note that expressions for the side chain length differ across the references (M, n, N_s, L); N_{sc} is used here to maintain consistency with the terminology in this thesis.

Expression	Methods	References	Eq.
$\lambda_b \sim N_{sc}^{3/4}$	Scaling theory, Monte Carlo simulations	19–21	1-1
$\lambda_b \sim N_{sc}^{1}$	Static light scattering, Small-angle X-ray scattering	22–23	1-2
$\lambda_b \sim N_{sc}^{15/8}$	Scaling theory	1	1-3
$\lambda_b \sim N_{sc}^{2} / \ln N_{sc}$	Perturbation theory, Monte Carlo simulations	24	1-4
$\lambda_b \sim N_{sc}^{2}$	Perturbation theory, Static light scattering	25–28	1-5

Initial reports attributed the wide variation in v to the limitations of certain methods. However, later insights indicate that the apparent conflicts are not consequences of calculation or measurement errors: instead, the disparities reflect the existence of multiple conformational regimes in the bottlebrush parameter space.[9,29-30] In other words, the conformation (and therefore the physical properties) of a bottlebrush polymer depends on its unique combination of N_{bb}, N_{sc}, z, etc. Recent studies have proposed *universal* models for graft polymer conformation based on scaling analyses.[9,29-30] In one example, four distinct conformational regimes were proposed based on predicted relationships between the molecular structure and the plateau modulus, then mapped in terms of N_{sc} and the average backbone length between adjacent grafts ($N_g = 1/z$) (Figure 1.2A). Below a critical grafting density ($N_g > N_g^{**}$), loose comb (LC), dense comb (DC), and loose brush (LB) regimes are anticipated as functions of N_{sc}. The comb regimes exhibit unperturbed Gaussian backbones and side chains, whereas LB marks the onset of backbone stretching due to side chain crowding. Above the critical grafting density ($N_g < N_g^{**}$), a dense brush (DB) regime is anticipated regardless of N_{sc}, in which both the backbones and side chains are extended. Figure 1.2B provides the corresponding scaling predictions for the entanglement plateau modulus ($G_{e,graft}$) of graft polymer melts relative to linear melts ($G_{e,linear}$) as a function of N_{sc}.

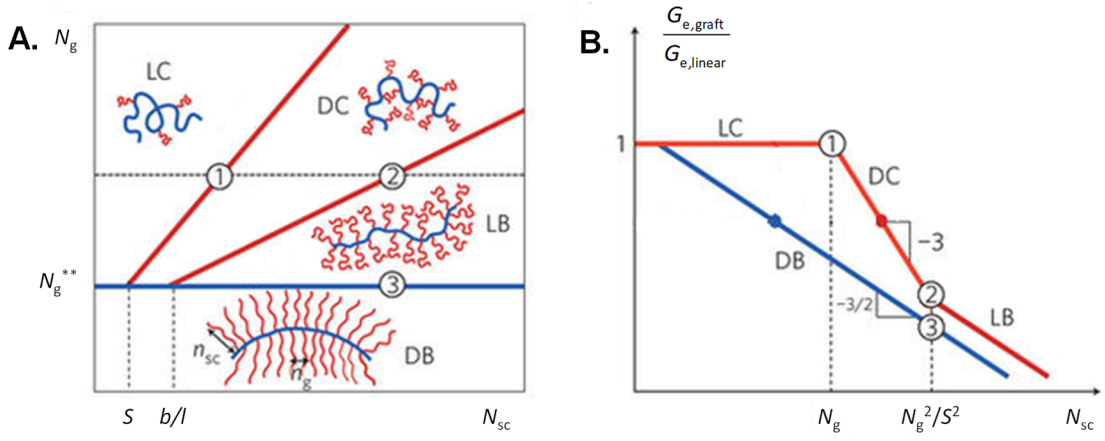

Figure 1.2: (*A*) Diagram of states for graft polymers based on the side chain degree of polymerization (N_{sc}) and inverse grafting density ($N_g = 1/z$). Loose comb (LC), dense comb (DC), loose brush (LB), and dense brush (DB) regimes are anticipated by theory. The conformations of the side chains and backbone vary in each regime. (*B*) Predicted entanglement plateau modulus of graft polymer melts ($G_{e,graft}$) relative to linear polymer melts ($G_{e,linear}$) as a function of N_{sc}. The normalized modulus decreases with increasing N_{sc}, and the scaling exponent changes in each regime. Adapted with permission from Ref. 9.

The predictions in Figure 1.2 reinforce the intimate connections between polymer conformation and physical properties. The predictions also highlight the need for additional studies. Recent computer simulations support the mapping of four distinct conformational regimes onto the molecular parameter space,[29-30] but the locations of the boundaries between regimes and the expected physical behavior in each regime remain topics of ongoing debate. In other words: for any backbone and side chain chemistries and any chain dimensions, what distinguishes bottlebrush polymers from other graft polymers? How do the physical properties vary in the bottlebrush regime?

Furthermore, any universal model for graft polymer conformation must be consistent with experimental measurements. However, experimental studies remain limited due to long-standing synthetic challenges associated with preparing well-defined model systems. Achieving precise control over key structural parameters — N_{bb}, N_{sc}, z, and the graft distribution — while maintaining narrow dispersity and enabling systematic variations presents significant challenges. This thesis will first describe our work to improve control over the graft polymer architecture (Chapter 2), then explore the physical consequences of polymer architecture in various contexts (Chapters 3–6). In order to motivate the challenges and opportunities for molecular design, the next section of this introduction will review existing synthetic routes to bottlebrush polymers.

1-2 Bottlebrush Polymer Synthesis

Bottlebrush polymers present unique synthetic challenges due to the steric demands imposed by the densely grafted architecture. Despite these challenges, advances in controlled polymerization[31-34] have enabled several routes to well-defined bottlebrush polymers. Several excellent reviews have catalogued these synthetic strategies.[35-38] This section will provide a brief overview, then introduce our approach.

Bottlebrush polymers can be synthesized according to one of three strategies: grafting-to, grafting-from, and grafting-through (Figure 1.3). Each strategy offers distinct advantages and disadvantages toward molecular design.

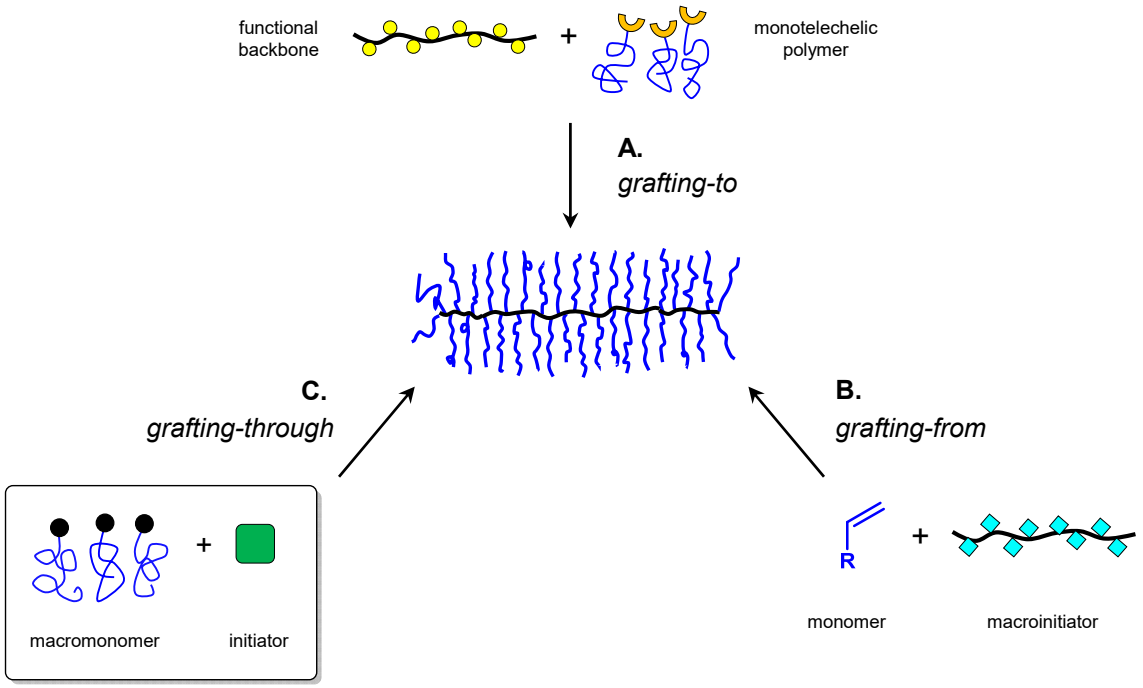

Figure 1.3: Three routes to synthesize bottlebrush polymers. (*A*) Grafting-to strategies attach monotelechelic chains to a pre-formed polymer backbone. (*B*) Grafting-from strategies grow side chains from a pre-formed macroinitiator. (*C*) Grafting-through strategies polymerize macromonomers in order to grow the brush through the backbone.

- The **grafting-to** approach attaches pre-formed monotelechelic chains to a pre-formed polymer backbone (Figure 1.3A). Grafting-to permits detailed characterization and modular variation of the side chains and backbone; however, steric demands typically limit the grafting density, result in non-uniform graft distributions, and require additional purification steps to remove unreacted chains.[39-42] Highly efficient coupling reactions (such as copper-catalyzed azide-alkyne click chemistry) can mitigate some of these limitations,[43-44] but in general high grafting densities ($z > 0.9$) can only be achieved with short side chains.
- The **grafting-from** approach grows side chains from a pre-formed macroinitiator (Figure 1.3B). Controlled radical polymerization enables the grafting-from synthesis of bottlebrushes with long backbones and narrow molecular weight distributions.[45-46] However, steric crowding typically limits the initiation efficiency along the backbone, leading to low grafting densities and non-uniform side chain

lengths.[47] In addition, determining z and N_{sc} is challenging, complicating the interpretation of molecular structure/property relationships.

- Lastly, the **grafting-through** approach grows the bottlebrush architecture through the backbone by polymerizing macromonomers (Figure 1.3C). Each macromonomer consists of a polymer chain with a polymerizable end group. In this way, grafting-through *guarantees* 100% grafting density and uniform side chain lengths. However, the inherently low concentration of polymerizable end groups typically limits the backbone degrees of polymerization that can be achieved.

In general, grafting-to and grafting-from strategies offer limited control over the side chain length, grafting density, and graft distribution due to steric crowding along the pre-formed backbone. In contrast, the grafting-through synthesis of bottlebrushes *guarantees* quantitative grafting density and uniform side chain lengths. Robust and efficient reactions are required in order to realize the full potential of the grafting-through approach. A wide variety of polymerization methods have been exploited, including atom-transfer radical polymerization (ATRP),[48-53] nitroxide-mediated polymerization (NMP),[54] anionic polymerization,[55-57] Suzuki polycondensation,[58-59] and cyclopolymerization of terminal diynes.[60] However, in many examples, the macromonomer synthesis is challenging, the functional group tolerance is limited, or only short backbone degrees of polymerization can be obtained.

Grafting-through ring-opening metathesis polymerization (ROMP) overcomes these limitations, providing a powerful route to well-defined graft polymers.[61-65] ROMP is a chain-growth polymerization in which cyclic monomers are opened and connected via the rearrangement of carbon-carbon double bonds (Scheme 1.1). Initiation occurs when a cyclic olefin monomer coordinates to the metal alkylidene catalyst. Subsequent [2+2] cycloaddition generates a metallacyclobutane intermediate, which then undergoes cycloreversion to produce a new olefin and a new metal alkylidene species. The high ring strain of the cyclic monomer disfavors unproductive cycloreversion and drives the reaction forward. Propagation occurs as these events are repeated until the monomer is completely consumed, equilibrium is reached, or termination occurs.

Scheme 1.1: Mechanism of ring-opening metathesis polymerization (ROMP). In well-defined catalysts, the metal center (M) is tungsten, molybdenum, or ruthenium.

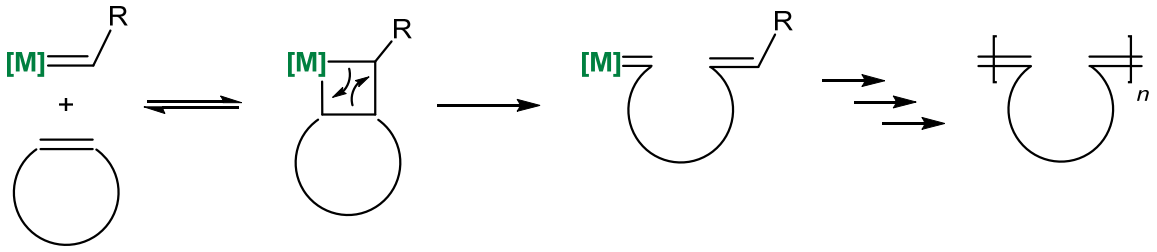

Judicious choice of the cyclic monomer and metathesis catalyst can achieve *living* ROMP. In a living polymerization, chain termination and chain transfer reactions are eliminated. As a result, living polymerizations generally exhibit a linear increase in molecular weight with conversion and a narrow molecular weight distribution ($Đ$ < 1.1).[61,66] This precision and control are highly desirable for materials design. In addition, the synthesis of well-defined model systems is crucial to enable the study of key structure-property relationships.

Norbornenes have emerged as the monomers of choice for living ROMP due to their high ring strain,[67] widespread commercial availability, and ease of functionalization. Early reports of grafting-through ROMP employed ω-norbornenyl macromonomers and a well-defined ruthenium or molybdenum metathesis catalyst;[68-72] however, these examples were not living due to the slow rate of initiation relative to propagation. Recent work has overcome this limitation by using the fast-initiating, highly active third-generation Grubbs catalyst, $(H_2IMes)(pyr)_2(Cl)_2Ru{=}CHPh$ (**G3**).[73-75] The living grafting-through ROMP of ω-norbornenyl macromonomers catalyzed by **G3** provides access to well-defined bottlebrush polymers (Figure 1.4). The macromonomers are connected one by one, stitching the bottlebrush architecture together through the backbone, until they are all consumed. Due to the high ring of norbornene and the high activity of **G3**, ultrahigh molecular weights (M_w > 4 MDa, N_{bb} > 1000) and excellent control over the molecular weight distribution ($Đ$ < 1.1) can be achieved.[76]

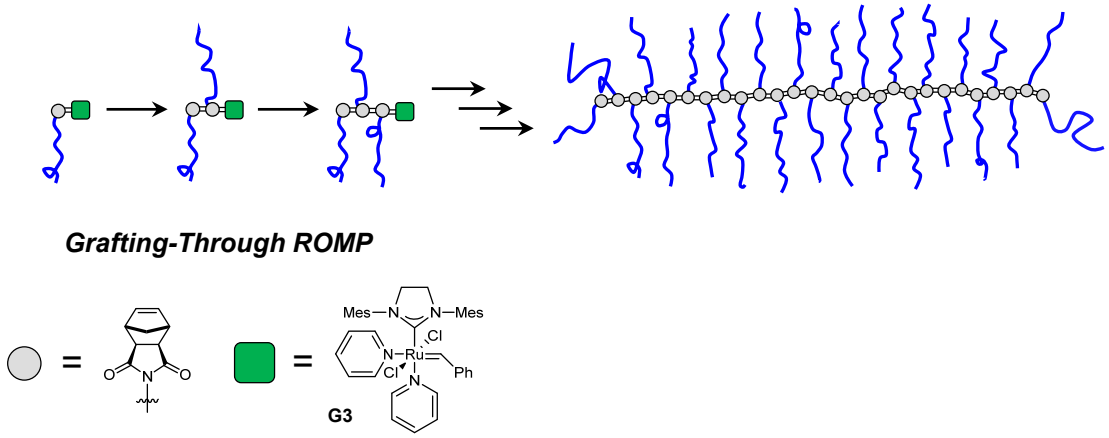

Figure 1.4: Living grafting-through ROMP of ω-norbornenyl macromonomers mediated by the fast-initiating **G3** catalyst. Macromonomers are stitched together through the backbone, providing access to well-defined bottlebrush polymers.

Living grafting-through ROMP enables precise, modular control over the graft polymer architecture. In the absence of termination events, ROMP proceeds until all of the macromonomer is consumed. At this point, even though propagation ceases, the catalyst is still active. The polymerization can be quenched to yield a bottlebrush *homopolymer* (Figure 1.5A); alternatively, a macromonomer with different side chain can be introduced, leading to AB bottlebrush *block polymers* (Figure 1.5B). The backbone degrees of polymerization for each block are directly determined by the macromonomer and catalyst stoichiometry: for example, given x equivalents of Macromonomer A and x equivalents of Macromonomer B relative to 1 equivalent of **G3**, $N_{bb,A} = N_{bb,B} = x$.

The relative block lengths can be changed simply by changing the macromonomer stoichiometry. Comparing Figure 1.5B–C, the *total* backbone degree of polymerization is fixed ($N_{bb} = N_{bb,A} + N_{bb,B} = 2x$), but the relative block lengths in Figure 1.5C differ by an increment of $2y$. The grafting-through strategy also permits varying the side chain length (N_{sc}) while fixing all other aspects of the molecular architecture, simply by changing the macromonomer molecular weight (Figure 1.5D).

Chapter 2 will describe an approach we developed to tune the grafting density and graft distribution. Compared to fully grafted bottlebrushes (Figure 1.5A–D), the grafting density can be lowered by copolymerizing macromonomers with small-molecule co-monomers (Figure 1.5E). These co-monomers "dilute" the grafting density by increasing

the number of backbone repeat units between grafts. In each block, if the macromonomer and diluent are similarly reactive, the graft distribution is uniform along the backbone (Figure 1.5E); if the relative reactivities differ, gradient or blocky distributions result (Figure 1.5F).

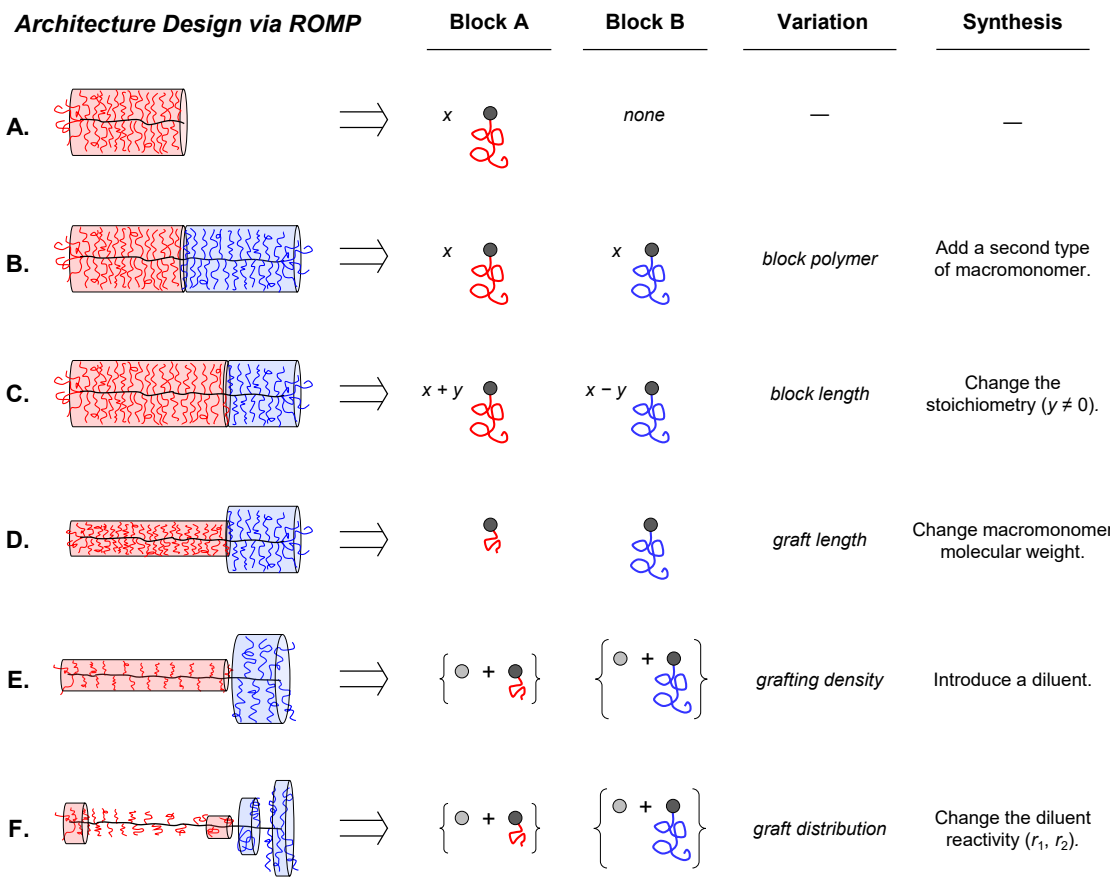

Figure 1.5: Opportunities for architectural design via living grafting-through ROMP. Schematic illustrations of polymer architectures are provided on the left. For ease of visualization, the polymers are illustrated in the limit of fully extended backbones, and cylinders indicate the anticipated local cross-sectional radii of gyration. Red and blue side chains indicate different chemical compositions (*i.e.*, Block A and Block B, respectively). For each row (B–F), the architectural variation compared to the previous row (*second to last column*) and required synthetic change (*last column*) are provided.

Living grafting-through ROMP emerges as a powerful route to well-defined bottlebrush polymers. The livingness of ROMP ensures low dispersity and enables tuning the backbone degrees of polymerization, while the grafting-through strategy guarantees fixed side chain degrees of polymerization and controlled grafting density. This exquisite

control over the molecular architecture enables the study of fundamental structure-property relationships as well as the design of functional materials.

Block polymers, such as those illustrated in Figure 1.5B–F, represent an attractive platform for materials design. Chapters 3–6 of this thesis will discuss our work to study the impact of molecular architecture on the properties and phase behavior of block polymers. Section 1-3 will provide an overview of key concepts in block polymer self-assembly.

1-3 Block Polymer Self-Assembly

Block polymers are advanced materials synthesized by joining two or more polymer chains of different chemical compositions. The chemical incompatibility between components favors minimizing the number of contacts and therefore the interfacial area. In simple mixtures of oil and water, this thermodynamic penalty to mixing drives *macrophase* separation. In contrast, in block polymers, the single covalent linkage between blocks constrains separation to the *nanoscale*. A rich variety of periodic nanostructures can result.[34,77-80]

For the simplest possible block architecture (a linear AB diblock polymer), three synthetic parameters influence self-assembly: (1) the total degree of polymerization, N; (2) the block volume fractions ($f_A = 1-f_B$); and (3) the free-energy penalty mixing blocks, χ_{AB}. Figure 1.6 illustrates the equilibrium morphologies commonly observed for linear AB diblock polymers: body-centered cubic spheres, hexagonally packed cylinders, gyroids, and lamellae.[81-83] Recent reports have also identified complex low-symmetry structures in linear AB diblock polymers, such as Frank-Kasper phases and quasicrystal approximants.[84-88] This diverse phase space highlights the potential of block polymer self-assembly to tune the composition, geometry, and length scales of materials.

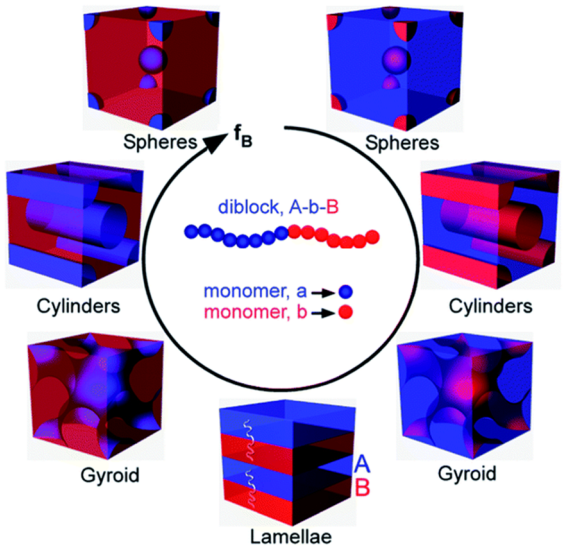

Figure 1.6: Equilibrium morphologies observed linear AB diblock polymers, the simplest polymer architecture. Reproduced with permission from Ref. 89.

The introduction of polymers with complex architectures creates additional opportunities for controlling self-assembly and properties. Graft polymers, due to their remarkable spatial dimensions and modular structures, offer several advantages for materials design. For example, due to steric-induced stiffening (Section 1-1), bottlebrush polymers display higher entanglement molecular weights,[4,9,90-91] lower melt viscosities,[3,92-93] and faster ordering kinetics[17,94] than their linear analogues. Recent reports have demonstrated that these unique dynamic properties enable bottlebrush block polymers to rapidly self-assemble to ultralarge domain sizes, on the order of the wavelength of visible light (d^* >100 nm) or even infrared radiation (d^* > 400 nm).[16-18,95] As a result, the bottlebrush architecture can enable the fabrication of materials that are generally inaccessible using linear polymers and other low-z analogues.

Figure 1.7 compiles examples of the relationship between d^* and the total backbone degree of polymerization (N_{bb}) for fully grafted bottlebrush diblock polymers. All brush diblock polymers feature poly(D,L-lactide) (PLA) and polystyrene (PS) side chains of similar molecular weights. In addition, all polymers were processed in the same way (*i.e.*, by thermal annealing) and assemble to long-range-ordered lamellar structures. Living grafting-through ROMP allows N_{bb} to be tuned over a wide range ($10 < N_{bb} < 1000$), which in turn enables control over d^* ($10 < d^* < 1000$).

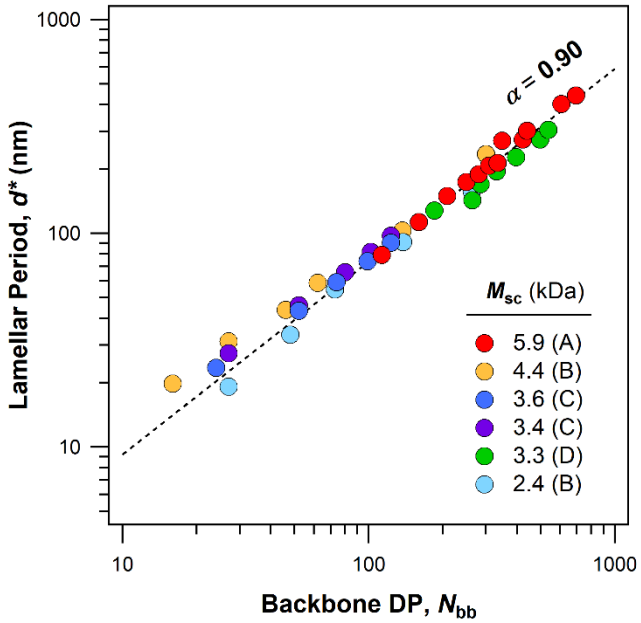

Figure 1.7: Compiled reported examples of the scaling of the lamellar period (d^*) with the backbone length (N_{bb}) for six series of bottlebrush diblock polymers. All polymers are fully grafted and feature symmetric PLA and PS side chains. The average side chain molecular weights (M_{sc}, in kDa) are provided in the legend. The letters in parentheses indicate the corresponding reference: (*A*) = Ref. 17, (*B*) = Ref. 94, (*C*) = Ref. 96, and (*D*) = Ref. 97. A dotted line corresponding to $\alpha = 0.90$ is included for comparison.

Figure 1.8 compares the self-assembly of linear ($z = 0$) and fully grafted bottlebrush ($z = 1$) block polymers to lamellar morphologies. For symmetric linear diblock polymers, arguments based on free energy demands accurately predict the scaling behavior ($d^* \sim N_{bb}^{\alpha}$). The scaling exponent α is 1/2 in the weak segregation limit ($\chi N_{bb} \approx 10.5$) and plateaus at 2/3 in the strong segregation limit ($\chi N_{bb} >> 10.5$).[83,98] The small scaling exponent is inherently related to the coil-like chain conformations. In contrast, bottlebrush block polymers display much larger scaling exponents ($\alpha = 0.8–0.9$),[16-17,94,99] consistent with their extended, wormlike backbone conformations. Understanding the connections between the molecular architecture, physical properties, and self-assembled structure will create further opportunities for materials design.

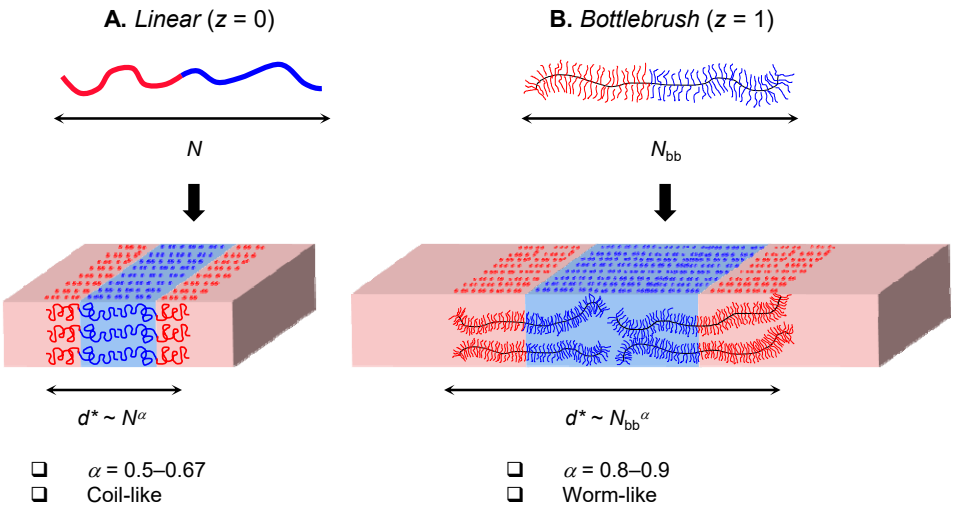

Figure 1.8: Self-assembly of (*A*) linear and (*B*) bottlebrush diblock polymers to lamellar morphologies. The scaling of the lamellar period with backbone degree of polymerization ($d^* \sim N_{bb}^{\alpha}$) differs as a consequence of the molecular architecture.

1-4 Thesis Outline

This thesis presents our work studying the impact of the graft polymer architecture on block polymer self-assembly. Our work connects (1) the synthesis of polymers with precisely tailored molecular architectures, (2) the study of fundamental structure-property relationships, and (3) the design of functional materials.

All of the work described in this thesis has been crucially enabled by robust chemistry — that is, by our ability to synthesize well-defined polymers by ring-opening metathesis polymerization (ROMP). In order to highlight the central role of chemistry, this thesis is not structured in chronological order. Instead, we will first discuss our recent contributions to expanding the ROMP synthetic method (Chapter 2). Copolymerizing a macromonomer and a small-molecule co-monomer provides access to well-defined polymers spanning the linear, comb, and bottlebrush regimes.

The synthetic advances introduced in Chapter 2 enable systematic variations of the grafting density, graft distribution, and backbone degrees of polymerization. In Chapter 3, we will explore the physical consequences of these architectural variations in two contexts: block polymer self-assembly and linear rheological properties. Chapters 4 and 5 discuss the phase behavior of fully grafted ABC bottlebrush triblock terpolymers featuring low-χ

interactions between the end blocks. The interplay of low-χ design and the molecular architecture reveals competing influences, which emerge in our discovery of a unique partially mixed lamellar morphology (LAM$_P$) and other physical consequences. Lastly, Chapter 6 describes applications of bottlebrush polymers as functional materials. Self-assembly enables mesoscale structural control over many materials properties, such as reflectivity, conductivity, and modulus. Collectively, our work creates new opportunities for molecular and materials design.

1-5 References

(1) Fredrickson, G. H. *Macromolecules* **1993**, *26*, 2825–2831.
(2) Mikhaylov, I. V.; Darinskii, A. A. *Polym. Sci. Ser. A* **2015**, *57*, 239–250.
(3) Dalsin, S. J.; Hillmyer, M. A.; Bates, F. S. *ACS Macro Lett.* **2014**, *3*, 423–427.
(4) Dalsin, S. J.; Hillmyer, M. A.; Bates, F. S. *Macromolecules* **2015**, *48*, 4680–4691.
(5) López-Barrón, C. R.; Brant, P.; Eberle, A. P. R.; Crowther, D. J. *J. Rheol.* **2015**, *59*, 865–883.
(6) Pakula, T.; Zhang, Y.; Matyjaszewski, K.; Lee, H.-i.; Boerner, H.; Qin, S.; Berry, G. C. *Polymer* **2006**, *47*, 7198–7206.
(7) Cai, L.-H.; Kodger, T. E.; Guerra, R. E.; Pegoraro, A. F.; Rubinstein, M.; Weitz, D. A. *Adv. Mater.* **2015**, *27*, 5132–5140.
(8) Vatankhah-Varnoosfaderani, M.; Daniel, W. F. M.; Zhushma, A. P.; Li, Q.; Morgan, B. J.; Matyjaszewski, K.; Armstrong, D. P.; Spontak, R. J.; Dobrynin, A. V.; Sheiko, S. S. *Adv. Mater.* **2017**, *29*, 1604209.
(9) Daniel, W. F. M.; Burdynska, J.; Vatankhah-Varnoosfaderani, M.; Matyjaszewski, K.; Paturej, J.; Rubinstein, M.; Dobrynin, A. V.; Sheiko, S. S. *Nat. Mater.* **2016**, *15*, 183–189.
(10) Lee, S.; Spencer, N. D. *Science* **2008**, *319*, 575–576.
(11) Bolton, J.; Bailey, T. S.; Rzayev, J. *Nano Lett.* **2011**, *11*, 998–1001.
(12) Ahn, S.-k.; Carrillo, J.-M. Y.; Keum, J. K.; Chen, J.; Uhrig, D.; Lokitz, B. S.; Sumpter, B. G.; Michael Kilbey, S. *Nanoscale* **2017**, *9*, 7071–7080.
(13) Bates, C. M.; Chang, A. B.; Momčilović, N.; Jones, S. C.; Grubbs, R. H. *Macromolecules* **2015**, *48*, 4967–4973.
(14) Bates, C. M.; Chang, A. B.; Schulze, M. W.; Momčilović, N.; Jones, S. C.; Grubbs, R. H. *J. Polym. Sci., Part B: Polym. Phys.* **2016**, *54*, 292–300.
(15) McNicholas, B. J.; Blakemore, J. D.; Chang, A. B.; Bates, C. M.; Kramer, W. W.; Grubbs, R. H.; Gray, H. B. *J. Am. Chem. Soc.* **2016**, *138*, 11160–11163.
(16) Rzayev, J. *Macromolecules* **2009**, *42*, 2135–2141.
(17) Sveinbjörnsson, B. R.; Weitekamp, R. A.; Miyake, G. M.; Xia, Y.; Atwater, H. A.; Grubbs, R. H. *Proc. Natl. Acad. Sci. U.S.A.* **2012**, *109*, 14332–14336.

(18) Miyake, G. M.; Weitekamp, R. A.; Piunova, V. A.; Grubbs, R. H. *J. Am. Chem. Soc.* **2012**, *134*, 14249–14254.
(19) Birshtein, T. M.; Borisov, O. V.; Zhulina, Y. B.; Khokhlov, A. R.; Yurasova, T. A. *Polym. Sci. U.S.S.R.* **1987**, *29*, 1293–1300.
(20) Saariaho, M.; Ikkala, O.; Szleifer, I.; Erukhimovich, I.; ten Brinke, G. *J. Chem. Phys.* **1997**, *107*, 3267–3276.
(21) Saariaho, M.; Szleifer, I.; Ikkala, O.; Brinke, G. t. *Macromol. Theory Simul.* **1998**, *7*, 211–216.
(22) Kikuchi, M.; Lien, L. T. N.; Narumi, A.; Jinbo, Y.; Izumi, Y.; Nagai, K.; Kawaguchi, S. *Macromolecules* **2008**, *41*, 6564–6572.
(23) Kikuchi, M.; Nakano, R.; Jinbo, Y.; Saito, Y.; Ohno, S.; Togashi, D.; Enomoto, K.; Narumi, A.; Haba, O.; Kawaguchi, S. *Macromolecules* **2015**, *48*, 5878–5886.
(24) Subbotin, A.; Saariaho, M.; Stepanyan, R.; Ikkala, O.; ten Brinke, G. *Macromolecules* **2000**, *33*, 6168–6173.
(25) Saariaho, M.; Subbotin, A.; Szleifer, I.; Ikkala, O.; ten Brinke, G. *Macromolecules* **1999**, *32*, 4439–4443.
(26) Subbotin, A.; Saariaho, M.; Ikkala, O.; ten Brinke, G. *Macromolecules* **2000**, *33*, 3447–3452.
(27) Nakamura, Y.; Norisuye, T. *Polym J* **2001**, *33*, 874–878.
(28) Hatanaka, Y.; Nakamura, Y. *Polymer* **2013**, *54*, 1538–1542.
(29) Paturej, J.; Sheiko, S. S.; Panyukov, S.; Rubinstein, M. *Sci. Adv.* **2016**, *2*, e1601478.
(30) Liang, H.; Cao, Z.; Wang, Z.; Sheiko, S. S.; Dobrynin, A. V. *Macromolecules* **2017**, *50*, 3430–3437.
(31) Hadjichristidis, N.; Pitsikalis, M.; Pispas, S.; Iatrou, H. *Chem. Rev.* **2001**, *101*, 3747–3792.
(32) Polymeropoulos, G.; Zapsas, G.; Ntetsikas, K.; Bilalis, P.; Gnanou, Y.; Hadjichristidis, N. *Macromolecules* **2017**, *50*, 1253–1290.
(33) Matyjaszewski, K.; Tsarevsky, N. V. *Nature Chem.* **2009**, *1*, 276–288.
(34) Bates, C. M.; Bates, F. S. *Macromolecules* **2017**, *50*, 3–22.
(35) Zhang, M.; Müller, A. H. E. *J. Polym. Sci., Part A: Polym. Chem.* **2005**, *43*, 3461–3481.
(36) Sheiko, S. S.; Sumerlin, B. S.; Matyjaszewski, K. *Prog. Polym. Sci.* **2008**, *33*, 759–785.
(37) Verduzco, R.; Li, X.; Pesek, S. L.; Stein, G. E. *Chem. Soc. Rev.* **2015**, *44*, 2405–2420.
(38) Müllner, M.; Müller, A. H. E. *Polymer* **2016**, *98*, 389–401.
(39) Schappacher, M.; Deffieux, A. *Macromolecules* **2005**, *38*, 7209–7213.
(40) Gao, H.; Matyjaszewski, K. *J. Am. Chem. Soc.* **2007**, *129*, 6633–6639.
(41) Lanson, D.; Ariura, F.; Schappacher, M.; Borsali, R.; Deffieux, A. *Macromolecules* **2009**, *42*, 3942–3950.
(42) Chen, P.; Li, C.; Liu, D.; Li, Z. *Macromolecules* **2012**, *45*, 9579–9584.
(43) Engler, A. C.; Lee, H. i.; Hammond, P. T. *Angew. Chem., Int. Ed.* **2009**, *48*, 9334–9338.
(44) De, S.; Khan, A. *Chem. Commun.* **2012**, *48*, 3130–3132.
(45) Beers, K. L.; Gaynor, S. G.; Matyjaszewski, K.; Sheiko, S. S.; Möller, M. *Macromolecules* **1998**, *31*, 9413–9415.

(46) Börner, H. G.; Duran, D.; Matyjaszewski, K.; da Silva, M.; Sheiko, S. S. *Macromolecules* **2002**, *35*, 3387–3394.
(47) Sumerlin, B. S.; Neugebauer, D.; Matyjaszewski, K. *Macromolecules* **2005**, *38*, 702–708.
(48) Shinoda, H.; Matyjaszewski, K. *Macromolecules* **2001**, *34*, 6243–6248.
(49) Börner, H. G.; Matyjaszewski, K. *Macromol. Symp.* **2002**, *177*, 1–16.
(50) Chul, H. S.; Shijun, J.; Mircea, T.; Tomasz, K.; Krzysztof, M.; C., G. A.; Maurice, B. *J. Polym. Sci., Part A: Polym. Chem.* **2002**, *40*, 2736–2749.
(51) Neugebauer, D.; Zhang, Y.; Pakula, T.; Sheiko, S. S.; Matyjaszewski, K. *Macromolecules* **2003**, *36*, 6746–6755.
(52) Shinoda, H.; Matyjaszewski, K.; Okrasa, L.; Mierzwa, M.; Pakula, T. *Macromolecules* **2003**, *36*, 4772–4778.
(53) Neugebauer, D.; Zhang, Y.; Pakula, T. *J. Polym. Sci., Part A: Polym. Chem.* **2006**, *44*, 1347–1356.
(54) Hawker, C. J.; Mecerreyes, D.; Elce, E.; Dao, J.; Hedrick, J. L.; Barakat, I.; Dubois, P.; Jérôme, R.; Volksen, W. *Macromol. Chem. Phys.* **1997**, *198*, 155–166.
(55) Ederle, Y.; Isel, F.; Grutke, S.; Lutz, P. J. *Macromol. Symp.* **1998**, *132*, 197–206.
(56) Pantazis, D.; Chalari, I.; Hadjichristidis, N. *Macromolecules* **2003**, *36*, 3783–3785.
(57) Koji, I.; Junichiro, S. *J. Appl. Polym. Sci.* **2003**, *87*, 1790–1793.
(58) Sheng, Z.; Yu, Z.; Haijian, T.; Yufeng, Z.; Yu, P.; Feng, Z.; Qikai, Z.; Zhihao, S.; Xinghe, F. *J. Polym. Sci., Part A: Polym. Chem.* **2014**, *52*, 1519–1524.
(59) Zeigler, D. F.; Mazzio, K. A.; Luscombe, C. K. *Macromolecules* **2014**, *47*, 5019–5028.
(60) Kang, E.-H.; Lee, I.-H.; Choi, T.-L. *ACS Macro Lett.* **2012**, *1*, 1098–1102.
(61) Bielawski, C. W.; Grubbs, R. H. *Prog. Polym. Sci.* **2007**, *32*, 1–29.
(62) Leitgeb, A.; Wappel, J.; Slugovc, C. *Polymer* **2010**, *51*, 2927–2946.
(63) Sutthasupa, S.; Shiotsuki, M.; Sanda, F. *Polym. J.* **2010**, *42*, 905–915.
(64) Martinez, H.; Ren, N.; Matta, M. E.; Hillmyer, M. A. *Polym. Chem.* **2014**, *5*, 3507–3532.
(65) Grubbs, R. H.; Khosravi, E. *Handbook of Metathesis: Polymer Synthesis*; Wiley, 2015.
(66) Matyjaszewski, K. *Macromolecules* **1993**, *26*, 1787–1788.
(67) Schleyer, P. v. R.; Williams, J. E.; Blanchard, K. R. *J. Am. Chem. Soc.* **1970**, *92*, 2377–2386.
(68) Breunig, S.; Héroguez, V.; Gnanou, Y.; Fontanille, M. *Macromol. Symp.* **1995**, *95*, 151–166.
(69) Heroguez, V.; Breunig, S.; Gnanou, Y.; Fontanille, M. *Macromolecules* **1996**, *29*, 4459–4464.
(70) Mecerreyes, D.; Dahan, D.; Lecomte, P.; Dubois, P.; Demonceau, A.; Noels, A. F.; Jérôme, R. *J. Polym. Sci., Part A: Polym. Chem.* **1999**, *37*, 2447–2455.
(71) Allcock, H. R.; de Denus, C. R.; Prange, R.; Laredo, W. R. *Macromolecules* **2001**, *34*, 2757–2765.
(72) Jha, S.; Dutta, S.; Bowden, N. B. *Macromolecules* **2004**, *37*, 4365–4374.
(73) Bielawski, C. W.; Grubbs, R. H. *Angew. Chem., Int. Ed.* **2000**, *39*, 2903–2906.
(74) Choi, T.-L.; Grubbs, R. H. *Angew. Chem. Int. Ed.* **2003**, *42*, 1743–1746.
(75) Xia, Y.; Kornfield, J. A.; Grubbs, R. H. *Macromolecules* **2009**, *42*, 3761–3766.

(76) Haugan, I. N.; Maher, M. J.; Chang, A. B.; Lin, T.-P.; Grubbs, R. H.; Hillmyer, M. A.; Bates, F. S. *ACS Macro Lett.* **2018**, *7*, 525–530.
(77) Bates, F. S.; Fredrickson, G. H. *Phys. Today* **1999**, *52*, 32–38.
(78) Bates, F. S.; Fredrickson, G. H. *Annu. Rev. Phys. Chem.* **1990**, *41*, 525–557.
(79) Park, C.; Yoon, J.; Thomas, E. L. *Polymer* **2003**, *44*, 6725–6760.
(80) Bates, F. S.; Hillmyer, M. A.; Lodge, T. P.; Bates, C. M.; Delaney, K. T.; Fredrickson, G. H. *Science* **2012**, *336*, 434–440.
(81) Leibler, L. *Macromolecules* **1980**, *13*, 1602–1617.
(82) Khandpur, A. K.; Foerster, S.; Bates, F. S.; Hamley, I. W.; Ryan, A. J.; Bras, W.; Almdal, K.; Mortensen, K. *Macromolecules* **1995**, *28*, 8796–8806.
(83) Matsen, M. W.; Bates, F. S. *Macromolecules* **1996**, *29*, 1091–1098.
(84) Lee, S.; Bluemle, M. J.; Bates, F. S. *Science* **2010**, *330*, 349–353.
(85) Gillard, T. M.; Lee, S.; Bates, F. S. *Proc. Natl. Acad. Sci. U.S.A.* **2016**, *113*, 5167–5172.
(86) Kim, K.; Schulze, M. W.; Arora, A.; Lewis, R. M.; Hillmyer, M. A.; Dorfman, K. D.; Bates, F. S. *Science* **2017**, *356*, 520–523.
(87) Lee, S.; Leighton, C.; Bates, F. S. *Proc. Natl. Acad. Sci. U.S.A.* **2014**, *111*, 17723–17731.
(88) Schulze, M. W.; Lewis, R. M.; Lettow, J. H.; Hickey, R. J.; Gillard, T. M.; Hillmyer, M. A.; Bates, F. S. *Phys. Rev. Lett.* **2017**, *118*, 207801.
(89) Hu, H.; Gopinadhan, M.; Osuji, C. O. *Soft Matter* **2014**, *10*, 3867–3889.
(90) Abbasi, M.; Faust, L.; Riazi, K.; Wilhelm, M. *Macromolecules* **2017**, *50*, 5964–5977.
(91) Hu, M.; Xia, Y.; McKenna, G. B.; Kornfield, J. A.; Grubbs, R. H. *Macromolecules* **2011**, *44*, 6935–6943.
(92) Jeong, S. H.; Kim, J. M.; Baig, C. *Macromolecules* **2017**, *50*, 4491–4500.
(93) Lohse, D. J.; Milner, S. T.; Fetters, L. J.; Xenidou, M.; Hadjichristidis, N.; Mendelson, R. A.; García-Franco, C. A.; Lyon, M. K. *Macromolecules* **2002**, *35*, 3066–3075.
(94) Gu, W.; Huh, J.; Hong, S. W.; Sveinbjornsson, B. R.; Park, C.; Grubbs, R. H.; Russell, T. P. *ACS Nano* **2013**, *7*, 2551–2558.
(95) Runge, M. B.; Bowden, N. B. *J. Am. Chem. Soc.* **2007**, *129*, 10551–10560.
(96) Lin, T.-P.; Chang, A. B.; Luo, S.-X.; Chen, H.-Y.; Lee, B.; Grubbs, R. H. *ACS Nano* **2017**, *11*, 11632–11641.
(97) Macfarlane, R. J.; Kim, B.; Lee, B.; Weitekamp, R. A.; Bates, C. M.; Lee, S. F.; Chang, A. B.; Delaney, K. T.; Fredrickson, G. H.; Atwater, H. A.; Grubbs, R. H. *J. Am. Chem. Soc.* **2014**, 17374–17377.
(98) Semenov, A. V. *Sov. Phys.-JETP (Engl. Transl.)* **1985**, *61*, 733–742.
(99) Xia, Y.; Olsen, B. D.; Kornfield, J. A.; Grubbs, R. H. *J. Am. Chem. Soc.* **2009**, *131*, 18525–18532.